STU

Dissertation Thesis Abstract
on

Shear strength of reinforced concrete cantilever slabs under concentrated load

Submitted in partial fulfilment of the requirements for the degree of Doctor of Philosophy

By

Aleksandar Vidaković

Department of Concrete Structures and Bridges
Faculty of Civil Engineering
Slovak University of Technology in Bratislava

November, 2022

STU

Dissertation Thesis has been prepared at:
Department of Concrete Structures and Bridges

Submitter: *Ing. Aleksandar Vidaković*
Department of Concrete Structures and Bridges
Faculty of Civil Engineering
Slovak University of Technology in Bratislava
Radlinského 11, 810 05 Bratislava

Supervisor: *prof. Ing. Jaroslav Halvonik, PhD.*
Department of Concrete Structures and Bridges
Faculty of Civil Engineering
Slovak University of Technology in Bratislava
Radlinského 11, 810 05 Bratislava

Readers: *prof. Ing. Martin Moravčík, PhD.*
Department of Structures and Bridges
Faculty of Civil Engineering
University of Žilina
Univerzitná 8215/1, 010 26 Žilina

doc. Ing. Radim Nečas, PhD.
Institute of Concrete and Masonry Structures
Faculty of Civil Engineering
Brno University of Technology
Veveří 331/95, 602 00 Brno

Ing. Andrej Bartók, PhD.
Department of Concrete Structures and Bridges
Faculty of Civil Engineering
Slovak University of Technology in Bratislava
Radlinského 11, 810 05 Bratislava

Dissertation Thesis Abstract was sent on: 14.11.2022

Dissertation Thesis Defence will be held on: 30.11.2022 at 10:00 at Department of Concrete Structures and Bridges, Faculty of Civil Engineering, Slovak University of Technology in Bratislava, Radlinského 11, 810 05 Bratislava.

prof. Ing. Stanislav Unčík, PhD.
Dean of Faculty of Civil Engineering

Contents

Chapter 1

Introduction

Reinforced concrete cantilever slabs without shear reinforcement are commonly used for deck slabs of existing box girder bridges. These slabs are subjected to concentrated loads and are among the most critical parts of the load-carrying capacity of bridges. The concentrated loads resulting from the wheel pressure of heavy vehicles may lead to potential flexural, shear or punching shear failures. In contrast with flexural failure (which is ductile), the shear failure is brittle and therefore undesirable.

1.1 Problem statement

A large number of existing bridges were designed according to design codes from the 1950s and 1960s. These bridges are still in service and are subjected to a constant increase of traffic loads (Leahy et al. [19]). Under the application of current load models according to the Eurocode 1 [7], concrete bridge members without shear reinforcement, as bridge deck slabs, often do not meet the current demands of shear design check according to Eurocode 2 [8]. Consequently, a higher shear reinforcement than actually provided is needed.

The shear capacity of members without shear reinforcement in present codes are based on empirical and semi-empirical expressions (Sigrist et al. [31], Muttoni and Fernández Ruiz [24]). For one-way shear these expressions originate from experiments made mainly on simply supported beams, subjected to four-point bending. The setup for punching shear experiments most often consist of a centric loaded isolated slab specimens supported on a column. These considerations are tremendously different from those of a cantilever slab loaded with a concentrated load, as a slab with a greater width has the ability to redistribute the load in transverse direction, which contributes to its resistance (Lantsoght et al. [17]). The knowledge obtained from these tests are therefore most often not directly applicable on bridge deck slabs.

Despite intensive research investigations in the last decade regarding shear strength of reinforced concrete cantilever slabs under concentrated loads (Vaz Rodrigues et al.

[32, 33], Rombach and Latte [30, 18], Reissen and Hegger [28, 27], Natário et al. [26, 25], Rombach and Henze [29]), the shear capacity of cantilever slabs without shear reinforcement has not yet been satisfactorily clarified.

Existing experimental database is still somewhat limited and along with missing model for the shear distribution in case of concentrated load, it became the major motivation for this research project.

1.2 Aims

The main aims of this thesis are:

- to investigate the shear behaviour of the reinforced concrete bridge deck slabs without shear reinforcement under concentrated load;
- to study the influence of the location of the concentrated load on shear capacity of the cantilever slabs;
- to evaluate the safety level of the current Eurocode 2 [8], the proposed revision of Eurocode 2 (prEN 1992-1-1:2021 [6]) and other relevant models for predicting the shear capacity and based on the analyses performed, to propose modifications of these models;
- to provide simple, consistent and rational design method for new structures and assessment of existing ones and therefore reduce the number of existing structures that need to be strengthened and retrofitted.

1.3 Objectives

In order to achieve the main aims of this thesis, the following set of objectives are stated:

- to perform an extensive literature study and collect the test results focused on the behaviour of cantilever slabs under concentrated load;
- to provide an experimental tests and increase the number of available tests on reinforced concrete cantilever slabs representing the deck slabs of bridges;
- to develop and demonstrate a non-linear finite element analysis model to predict the behaviour of the performed experimental tests;
- to perform parametric studies to investigate how, and to what degree, different parameters influence the internal forces redistributions in cantilever slabs under concentrated load.

Chapter 2

Literature review

A summary of a conducted literature study is presented in this chapter, which aims to give the state-of-the-art review on shear behaviour of reinforced concrete members without shear reinforcement.

2.1 Mechanisms of shear transfer

In reinforced concrete (RC) members with or without shear reinforcement, the external and internal shear forces must be in equilibrium. In general, the applied (external) shear force is resisted by a combination of all the internal forces acting as shear transfer mechanisms. A summary of these shear transfer mechanisms for a cracked reinforced concrete beam without shear reinforcement can be described in form of free body diagram presented in Figure 2.1, in which the following symbols are used:

- V_{cz} concrete compression zone;
- V_{cr} residual tensile strength;
- V_{ag} aggregate interlock;
- V_{da} dowel action.

These four mechanisms are referred as beam actions, as they allow carrying shear in member keeping constant lever arm between the tension and compression chord.

Other than beam actions, shear forces can be also transferred through arching (or strut) action assuming a constant force in the flexural reinforcement, leading to the plasticity-based stress field proposed by Drucker [10].

Shear behaviour and mode of failure of reinforced concrete members is highly affected by the shear span-to-depth ratio a/d. This ratio is often referred to as the shear slenderness. It was first investigated on beams by Leonhardt and Walther [20] and by Kani [14] who demonstrated it by the so-called 'Kani's valley' shown in Figure 2.2.

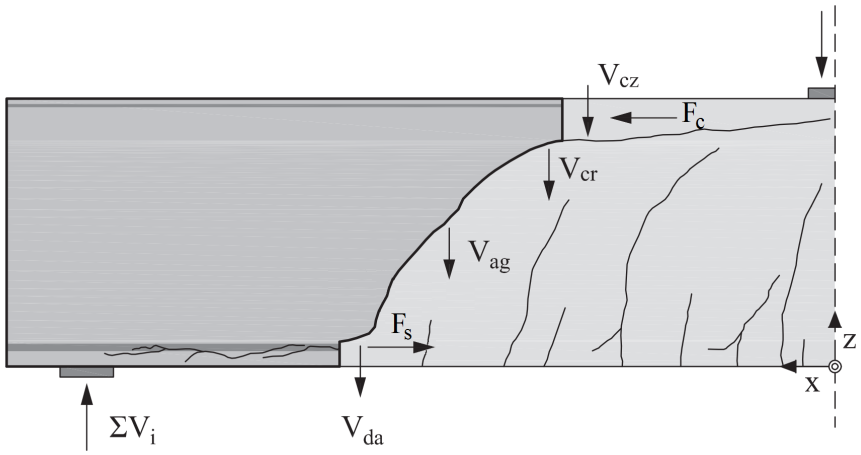

Figure 2.1: Mechanisms of shear transfer acting on the considered free body diagram defined by the critical shear crack.

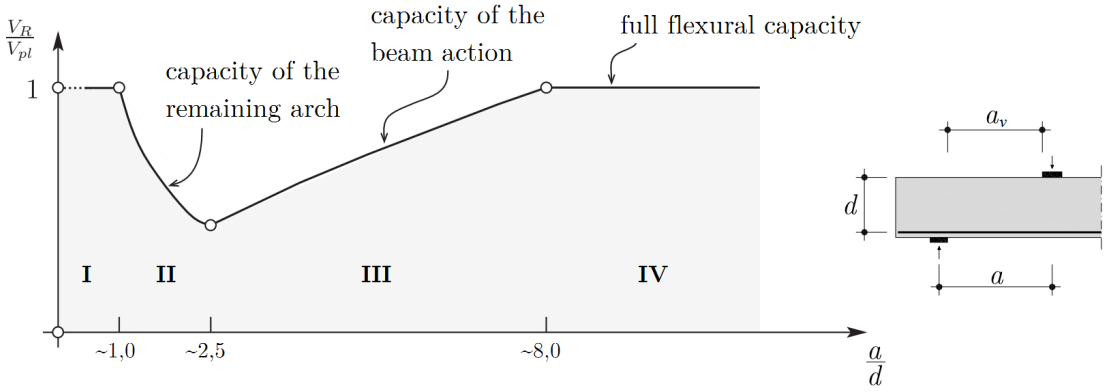

Figure 2.2: 'Kani's valley' (Kani et al. [15]).

If the shear span decreases below $a/d \lesssim 2.5$, arching action will develop and the shear strength capacity will increase. Compared to the arching action of beams, this increase in capacity is not as remarkable for slabs because the direct load transfer is counteracted by a decrease in effective shear width when the load acts closer to the support of a slab. The ratio between the bending moment and the shear force m/v for beams is directly proportional to the shear span-to-depth ratio a/d. This is, however, not the case for cantilever slabs under concentrated loads, where the ratio between the maximum acting bending moment and the maximum acting shear force m_{max}/v_{max} at the support is lower than for a beam with the same shear span. It was also observed by Lantsoght et al. [17] and Reissen and Hegger [28] that the shear capacity of slabs under concentrated loads with small shear span-to-depth ratio a/d is larger for clamped slabs than for the simply supported ones.

All these differences, thus, lead to the conclusion, that the influence of the location of the concentrated load on shear behaviour is different for the beams, clamped slabs (e.g. cantilever deck slabs of bridges) and one-way simply supported slabs.

Chapter 3

Analytical models for shear strength prediction

Analytical models for predicting shear strength of reinforced concrete members without shear reinforcement are presented. The scope of this chapter is not to give a complete overview of all the proposed models, but to briefly describe only the models that have influenced the approach of this thesis.

3.1 Critical Shear Crack Theory

The Critical Shear Crack Theory (CSCT) was originally developed by Muttoni [22] for punching shear design of slabs without shear reinforcement. It was later extended to slender reinforced concrete beams and one-way slabs without shear reinforcement (Muttoni and Fernández Ruiz [24]).

This theory proposes that the shear capacity of a member can be completely related to the crack width at a predefined critical control section. It assumes that the critical crack width w_{cr} is proportional to the product of the longitudinal strain in the control section depth ε times the effective flexural depth d:

$$w_{cr} \propto \varepsilon\, d \tag{3.1}$$

The following CSCT failure criterion has been proposed for the shear strength of one-way slabs per unit width:

$$v_c(\varepsilon) = \frac{d\sqrt{f_c}}{3} \frac{1}{1 + 120\frac{\varepsilon d}{16+d_g}} \tag{3.2}$$

where f_c is the concrete compressive strength (in [MPa]), d is the effective flexural depth (in [mm]), d_g is the maximum aggregate size (in [mm]) and should be taken

as zero for high-strength ($f_c > 60$ MPa) or light-weight concrete, and ε is the longitudinal strain evaluated at $0.6d$ from the outer compressive fibre considering a linear elastic behaviour for concrete in compression and neglecting its tensile strength. The longitudinal strain ε and the depth of the compression zone c are defined by:

$$\varepsilon = \frac{m}{d\rho E_s(d - c/3)} \frac{0.6d - c}{d - c} \tag{3.3}$$

$$c = d\rho \frac{E_s}{E_c} \left(\sqrt{1 + \frac{2E_c}{\rho E_s}} - 1 \right) \tag{3.4}$$

where m is the unitary acting bending moment, ρ is the longitudinal reinforcement ratio, E_s is the Young's modulus of reinforcing steel and E_c is the Young's modulus of concrete.

3.2 Compression Chord Capacity Model

The Compression Chord Capacity Model (CCCM) was developed from a more general model called Multi-Action Shear Model (MASM) by Marí et al. [21]. It considers that the shear strength (V_R) comprises the shear resisted in the uncracked compression head (V_c), the shear resisted across the web crack (V_w) and the shear resisted due to the dowel action of the longitudinal reinforcement (V_l). It provides explicit expressions for each of the shear-resisting component. The model considers that failure occurs when the principal stresses at one point of the compression chord, at the critical section defined in the MASM, reach the Kupfer and Gerstle's failure envelope [16].

This model was later extended to the case of slabs under concentrated load (Fernández et al. [12]). The main effects of the proximity of the load to the support, such as the increase in the neutral axis depth, the change in the angle of the critical shear crack, and the generation of the vertical stresses confining the compression chord, were taken into account and introduced into the equilibrium equations. These equations were solved iteratively and after a parametric and statistical study, a simplified expression for the shear strength of cantilever slabs under concentrated load was derived:

$$V_R = 0.3\zeta \left(\left(0.47 - 0.058 \frac{a_v}{d} \right) + \left(1 - \frac{a_v}{3d} \right)^2 \frac{x_0}{d} \right) (f_c)^{2/3} b_w d \tag{3.5}$$

$$\zeta = \frac{2}{\sqrt{1 + \frac{d}{200}}} \left(\frac{d}{a} \right)^{0.2} \geq 0.45 \tag{3.6}$$

where ζ is the parameter taking into account the size effect and the shear slenderness, x_0/d is the relative neutral axis depth of the member and b_w is the effective shear width of the member.

3.3 Code provisions

In codes of practice, the shear strength $V_{R,c}$ (in [kN]) of a reinforced concrete slabs is calculated by multiplying a unitary shear strength $v_{R,c}$ (in [kN/m]) by the assumed effective shear width b_w (in [m]) at the control section according to the relevant model:

$$V_{R,c} = v_{R,c}\, b_w \tag{3.7}$$

If the concentrated loads are applied relatively close to the support, an arching action (refer to Subsection **??** and Section **??**) may be taken into account in some codes of practice, by reducing the acting shear force V (or the unitary acting shear force v for the wide members) by a factor β according to the relevant model. This factor β is based on tests on beams by Leonhardt and Walther [20], and Kani [14], refer to 'Kani's valley' shown in Figure 2.2.

3.3.1 *fib* Model Code 2010

The *fib* Model Code 2010 [11] (MC2010) proposes three different methods for calculating one-way shear resistance of concrete slabs: Level I, Level II and Level IV approximations (Muttoni and Fernández Ruiz [23]), with complexity and accuracy increasing as the level rises. The shear strength formulation is based on the Simplified Modified Compression Field Theory (Bentz et al. [4]) and is given by:

$$V_{R,c} = k_v \sqrt{f_c}\, z b_w \tag{3.8}$$

where the lever arm (also known as the effective shear depth) z can be taken as $0.9d$ (d is the effective flexural depth), b_w is the effective shear width, f_c is the concrete compressive strength (in [MPa]) and the value of $\sqrt{f_c}$ shall not be taken as greater than 8 MPa.

For a Level II approximation (LoA II), k_v is determined as:

$$k_v = \frac{0.4}{1 + 1500\varepsilon_x} \frac{1300}{1000 + k_{dg} z} \quad z \text{ in [mm]} \tag{3.9}$$

$$\varepsilon_x = \frac{1}{2E_s a_s} \left(\frac{m}{z} + v \right) \tag{3.10}$$

where ε_x is the longitudinal strain at the mid-depth of the effective flexural depth in the control section and shall not exceed 0.003, E_s is the modulus of elasticity of reinforcing steel, a_s is the unitary flexural reinforcement area, m and v are respectively the unitary acting bending moment and shear force at assumed control section and k_{dg} is a parameter depending on the maximum aggregate size d_g:

$$k_{dg} = \frac{32}{16 + d_g} \geq 0.75 \quad d_g \text{ in [mm]} \tag{3.11}$$

For concrete compressive strengths greater than 70 MPa and light-weight concrete, d_g shall be taken as zero, in order to account for the loss of aggregate interlock in the cracks due to fracture of aggregate particles.

Arching action is accounted in *fib* Model Code 2010 [11] for concentrated loads applied within a distance of $d \leq a_v \leq 2d$ from the face of the support by reducing the unitary acting shear force v by a factor β:

$$\beta = \begin{cases} \dfrac{a_v}{2d} & \text{for } d \leq a_v \leq 2d \\ 0.5 & \text{for } a_v < d \end{cases} \tag{3.12}$$

3.3.2 Eurocode 2

The shear strength formulation according to current Eurocode 2 [8] (EC2) was empirically calibrated with experimental data through a statistical approach based on the work of Zsutty [35]. The shear strength is given by:

$$V_{R,c} = \left[C_{R,c} k (100 \rho_l f_c)^{1/3}\right] b_w d \geq 0.035 k^{3/2} \sqrt{f_c}\, b_w d \tag{3.13}$$

where $C_{R,c}$ is the empirical factor ($C_{R,c} = 0.18$), f_c is the concrete compressive strength (in [MPa]), d is the effective flexural depth, ρ_l is the longitudinal reinforcement ratio with a maximum value of 0.02 and b_w is the effective shear width. The size-effect parameter k can be determined as:

$$k = 1 + \sqrt{\frac{200}{d}} \leq 2 \quad d \text{ in [mm]} \tag{3.14}$$

For members with loads applied within a distance of $0.5d \leq a_v \leq 2d$ from the face of the support, the acting shear force V may be reduced by a factor β:

$$\beta = \begin{cases} \dfrac{a_v}{2d} & \text{for } 0.5d \leq a_v \leq 2d \\ 0.25 & \text{for } a_v < 0.5d \end{cases} \tag{3.15}$$

3.3.3 ACI 318-19

The American code ACI 318-19 [1] provides the shear capacity equation for slender reinforced concrete members, as follows:

$$V_{R,c} = 0.6643 \lambda_s \lambda (\rho)^{1/3} \sqrt{f_c} b_w d \tag{3.16}$$

where f_c is the concrete compressive strength (in [MPa]) and the value of $\sqrt{f_c}$ shall not be taken as greater than 8.3 MPa, ρ is the longitudinal reinforcement ratio, d is the effective flexural depth, b_w is the effective shear width and λ is the modification

factor used to account for the lower tensile-to-compressive strength ratio of light-weight concrete compared with normal-weight concrete (for normal-weight concrete $\lambda = 1.0$ shall be used).

Bažant's [2] size effect factor λ_s is also introduced in this model as follows:

$$\lambda_s = \sqrt{\frac{2}{1 + \frac{d}{254}}} \leq 1.0 \tag{3.17}$$

3.3.4 prEN 1992-1-1:2021

Shear design for structural members without shear reinforcement according to the current draft for the revision of Eurocode 2 is a simplified formulation based on the Critical Shear Crack Theory (Muttoni and Fernández Ruiz [24]). This model is very similar to the current Eurocode 2 model, however, important influencing parameters, such as size effect or the influence of the normal stress are considered differently. Furthermore, a dependence of the shear resistance on maximum aggregate size and on the bending moment has been implemented in order to take into account the favourable effect of the aggregate interlocking mechanisms that can be transferred in the failure-determining shear crack within defined limits of the shear slenderness.

One-way shear verification in slabs without reinforcement according to this model is based on a comparison of shear strength with shear stress:

$$\tau_{Ed} \leq \tau_{Rd,c} \tag{3.18}$$

The shear stress is averaged along the cross-section and defined as:

$$\tau_{Ed} = \frac{V_{Ed}}{b_w z} \tag{3.19a}$$

$$\tau_{Ed} = \frac{v_{Ed}}{z} \tag{3.19b}$$

where V_{Ed} is design shear force in linear members, is design shear force per unit width in planar members, b_w is the width of the cross-section and z is the inner lever arm for determining shear stresses, defined as $0.9d$, where d is the effective flexural depth related to the centroid of the flexural tension reinforcement.

The shear strength of members without shear reinforcement is defined as

$$\tau_{Rd,c} = 0.66\left(100\rho_l f_c \frac{d_{dg}}{d}\right)^{1/3} \geq \tau_{Rdc,min} \tag{3.20}$$

where the minimum shear strength $\tau_{Rdc,min}$ is

$$\tau_{Rdc,min} = 11\sqrt{\frac{f_c}{f_{yd}}\frac{d_{dg}}{d}} \tag{3.21}$$

where ρ_l is the longitudinal reinforcement ratio, f_c is the concrete cylinder compressive strength, f_{yd} is the design yield strength of the flexural reinforcement and d_{dg} is a size parameter describing the failure zone roughness ($d_{dg} = 16\,\text{mm} + D_{lower} \leq 40\,\text{mm}$ for $f_c \leq 60\,\text{MPa}$ and $d_{dg} = 16\,\text{mm} + D_{lower}(60/f_c)^4 \leq 40\,\text{mm}$ for $f_c > 60\,\text{MPa}$, with D_{lower} being the smallest value of the coarsest fraction of aggregates).

If a structural member features an effective shear span $a_{cs} < 4d$, the value of d can be substituted by $a_{v,\text{prEC2}}$ which is defined as

$$a_{v,\text{prEC2}} = \sqrt{\frac{a_{cs}}{4}d} \tag{3.22}$$

The effective shear span a_{cs} related to the control section is defined as

$$a_{cs} = \left|\frac{M_{Ed}}{V_{Ed}}\right| \geq d \tag{3.23}$$

for determining a_{cs}, two load cases need to be considered: on the one hand, the maximum shear force with simultaneous moment and, on the other hand, maximum bending moment with associated shear force.

3.4 Effective shear width in wide beams and slabs

In wide beams and slabs subjected to concentrated load, the width at the support that carries the shear loading needs to be estimated. This width is the effective shear width b_w.

The effective shear width b_w usually depends on the national practices (Lantsoght et al. [17]). French and Dutch models are introduced in Figure 3.1(a) and Figure 3.1(b), respectively. The distribution under 45° is measured from the outer edges of the loaded area in the case of French (Chauvel et al. [9]) and from the center of the loaded area in the case of Dutch model. However, the models work well for limited distance of the loaded area from a support. For longer distances the safety level of the models decreases due to the overestimation of the effective shear width b_w. Therefore, the maximum distance of the critical sections from the inner edge of loaded area has to be defined. In order to remain within the scope of the Eurocode 2, the maximum distance of $2d$ was proposed, as can be shown in Figure 3.2(a) and (b).

In Model Code 2010 [11], the effective shear width b_w is determined by the load distribution angle of 45° for clamped and 60° for simply supported slabs (Figure 3.3). The critical section is assumed at the smaller distance of d and $a_v/2$ from the face of a support. To avoid the problem with overestimation of b_w, Model Code 2010 also requires to check possible failure due to the punching.

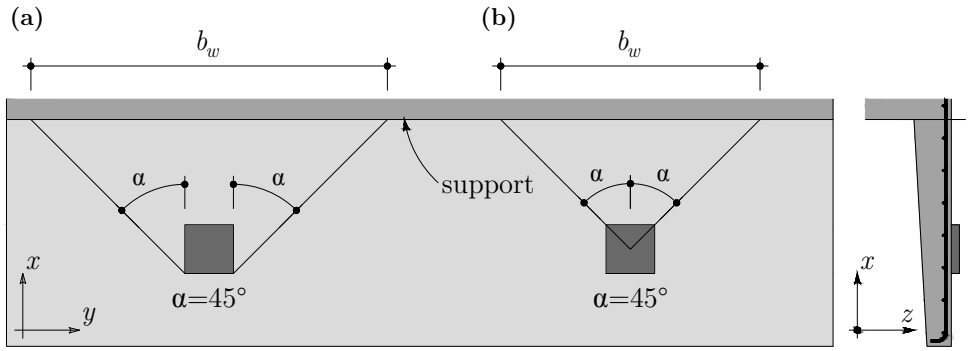

Figure 3.1: Effective shear width according to the: **(a)** French approach; and **(b)** Dutch approach.

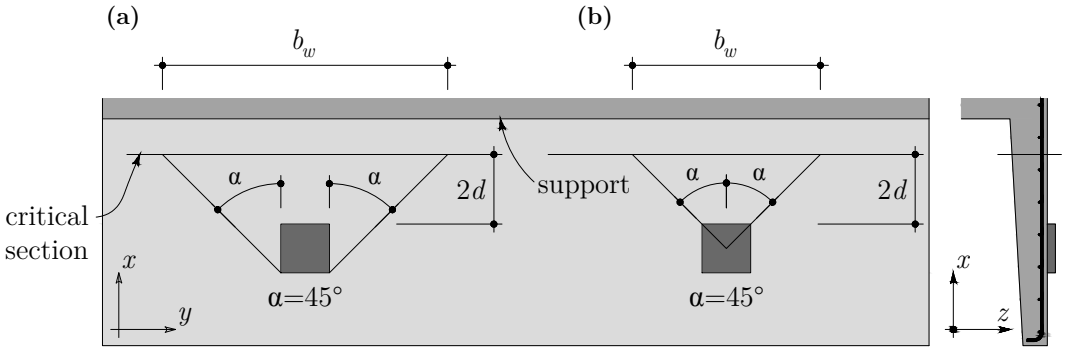

Figure 3.2: Proposed modification of the: **(a)** French approach; and **(b)** Dutch approach.

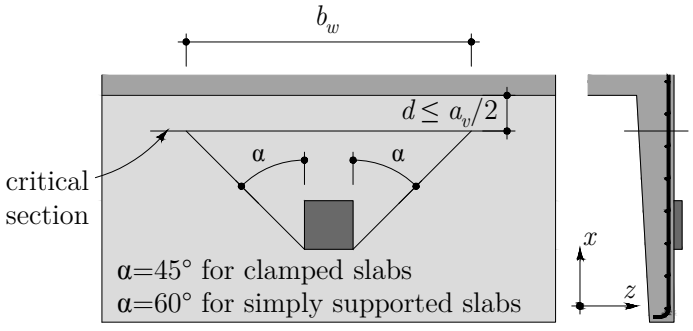

Figure 3.3: Effective shear width according to the Model Code 2010 [11].

In Compression Chord Capacity Model (CCCM), Fernández et al. [12] proposed the distribution angle of 52.5° and the critical section of cantilever slabs is assumed at the inner face of the loaded area by the distance βd (Figure 3.4). The distance βd is the horizontal projection of the first branch of the critical crack, in the tensile part of the slab, whose value is set by the geometrical assumptions. Assuming $\cot\theta = a_v/d$:

$$\beta d = (d - x_1)\cot\theta = \left(1 - \frac{x_1}{d}\right) a_v \tag{3.24}$$

where x_1 is the length of the uncracked zone, which is taken equal to the neutral axis depth. To account for the increment on the neutral axis depth x_1 due to the proximity of the load to the support, a parabolic variation of x_1 is assumed between $a_v/d = 3$, ($x_1 = x_0$, B-region) and $a_v/d = 0$ ($x_1 \approx 0.8d$), resulting in:

$$\frac{x_1}{d} = \frac{x_0}{d} + \left(0.8 - \frac{x_0}{d}\right)\left(1 - \frac{a_v/d}{3}\right)^2 \tag{3.25}$$

$$\frac{x_0}{d} = \rho\frac{E_s}{E_c}\left(\sqrt{1 + \frac{2E_c}{\rho E_s}} - 1\right) \tag{3.26}$$

where ρ is the longitudinal reinforcement ratio, E_s is the Young's modulus of reinforcing steel and E_c is the Young's modulus of concrete.

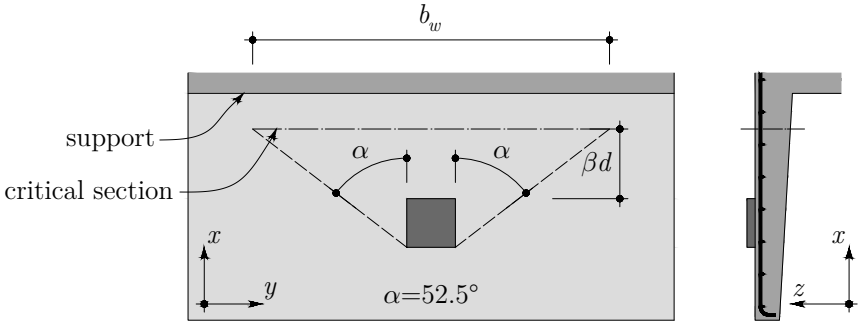

Figure 3.4: Effective shear width according to the CCCM.

Chapter 4

Experimental programme

In order to study the shear capacity or reinforced concrete cantilever slabs representing bridge deck slabs under concentrated load, five experimental specimens have been prepared. The experimental tests were carried out in the Structural Laboratory of the Slovak University of Technology in Bratislava.

4.1 Test procedure

4.1.1 Specimens

The geometry of the prepared cantilever slabs can be seen in Figure 4.1. The cantilever has a span of 1.6 m (distance from the fixed end to the tip of the cantilever) and a total length of 3 m. The slab has a constant thickness of 220 mm. The main reinforcement of the top layer at the fixed end consist of 16 mm diameter bars at 90 mm spacing, which corresponds to a reinforcement ratio of 1.20%. The transverse top reinforcement consists of 10 mm diameter bars at 90 mm spacing and the bottom reinforcement consists of 10 mm diameter bars at 125 mm spacing in both directions. The transverse reinforcement in form of 8 mm diameter bar stirrups was used in the cantilever on the backside to prevent the potential shear cracks in the 'passive' side of a cantilever. Figure 4.2 shows the reinforcement layout. The concrete cover is 25 mm. The effective flexural depth of all slab specimens is $d = 187$ mm.

4.1.2 Test set-up

Figure 4.3 shows the experimental set-up for a typical test. In order to distribute the concentrated load as uniformly as possible, it was applied in the symmetry axis through 10 mm thick neoprene pad using square steel plate with dimensions of 250 mm×250 mm×40 mm. It was applied by a hydraulic jack (with a total capacity of 1 MN) supported by a strong steel frame, which was anchored to the strong laboratory floor. At the interface between the concrete blocks and the tested slab

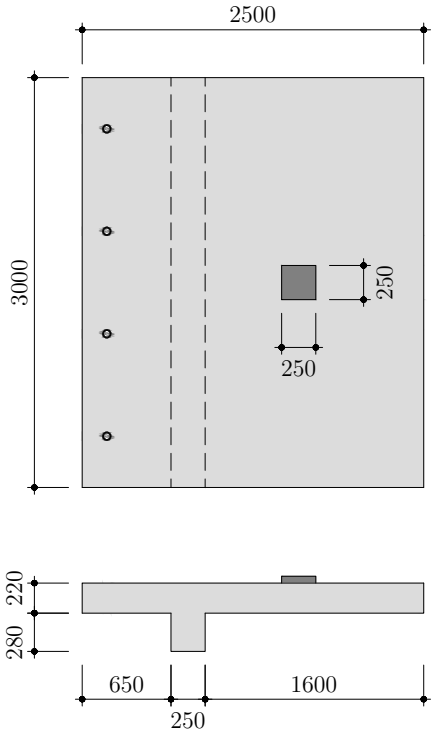

Figure 4.1: Geometry of the tested slab specimens (dimensions in [mm]).

specimen, there was a thin layer of mortar of about 5 mm, in order to get the levelled surfaces.

The cantilever on the backside was fixed by means of four vertically prestressed bars against the laboratory strong floor. Two UPN200 steel profiles were placed between the prestress bars and the slab specimen, in order to spread the prestress force uniformly along the slab width. A total prestress force of 2.4 MN was applied before the test.

Four different loading positions were investigated with a clear shear span-to-depth ratio of $a_v/d = 2$, 3, 4 and 5. Main properties of all tested specimens can be seen at Table 4.1.

Table 4.1: Properties of tested specimens.

Test	a_v [mm]	a_v/d	Age [days]	f_c [MPa]	E_c [GPa]
SP01	374	2	463	29.2	31.0
SP02	561	3	494	29.2	31.0
SP03	748	4	481	29.2	31.0
SP04A	935	5	225	29.0	31.0
SP04B	935	5	137	31.3	35.2

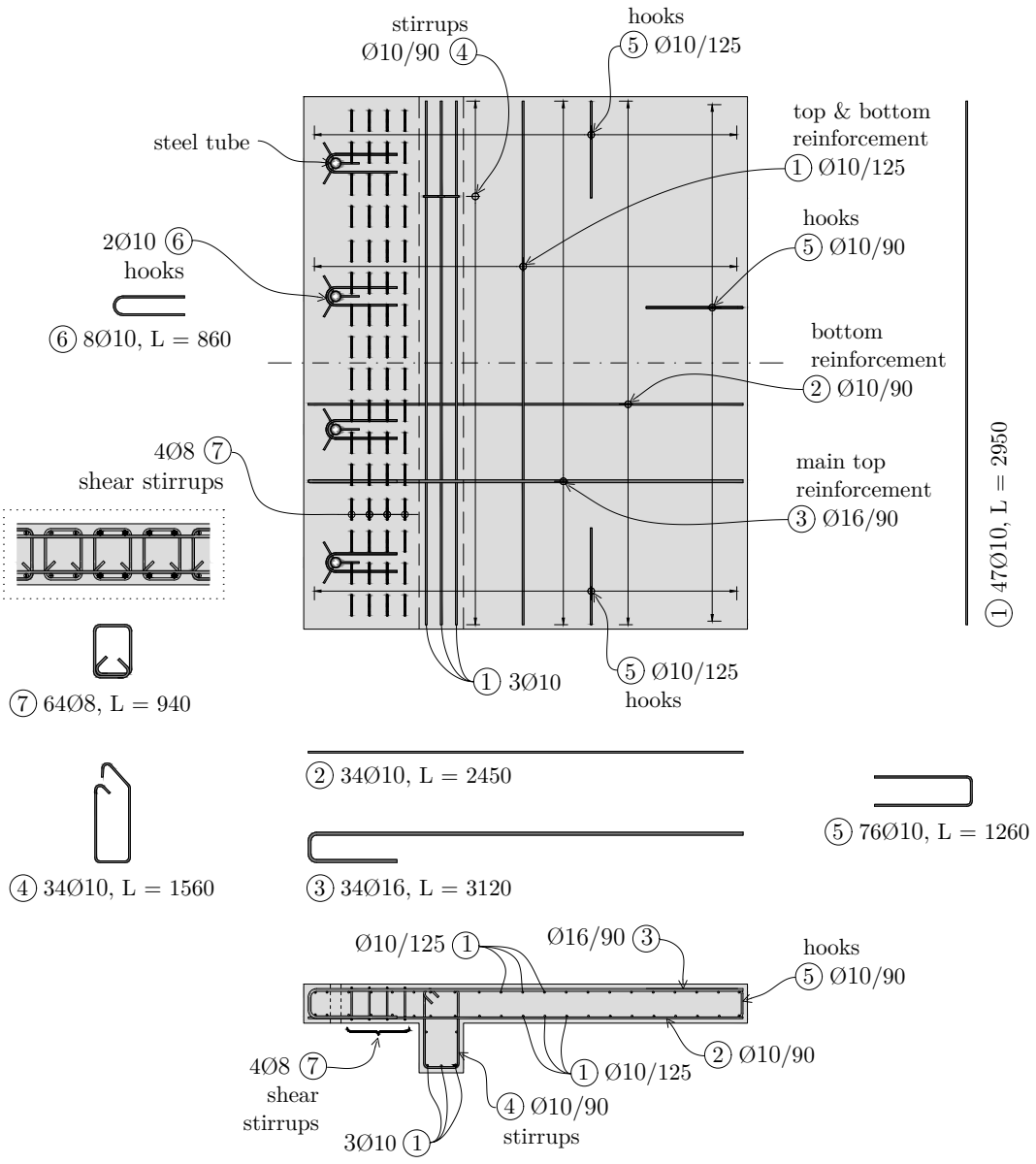

Figure 4.2: Reinforcement layout (dimensions in [mm]).

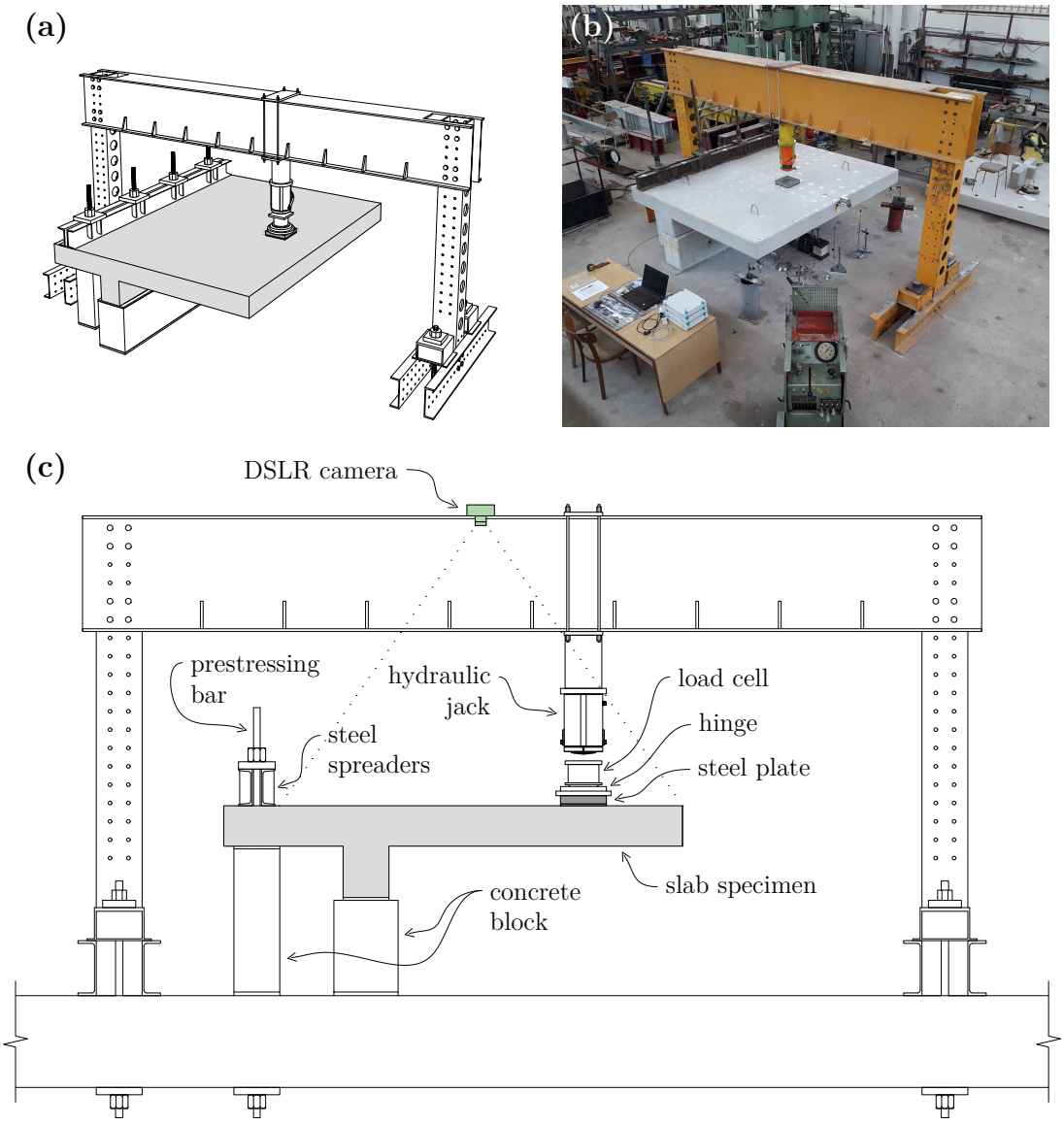

Figure 4.3: Experimental set-up: **(a)** perspective view; **(b)** photo; and **(c)** side view of the slab.

4.2 Test results

4.2.1 Load-displacement

Figure 4.4 shows the load-displacement curves for all slabs, where the displacement δ was measured at the center of the loading plate. A relatively constant value of the maximum load V_{max} is obtained with $a_v/d \geq 3$ (Table 4.2). The load bearing capacity is increased significantly for the slab specimen SP01 with $a_v/d = 2$.

Table 4.2: Measured maximum load and displacement (at the center of the loading plate) at failure for all specimens.

Test	a_v/d	V_{max} [kN]	$V_{max}/(d^2\sqrt{f_c})$	δ_{max} [mm]
SP01	2	621.2	3.29	9.98
SP02	3	444.6	2.35	11.87
SP03	4	470.5	2.49	15.95
SP04A	5	439.2	2.33	28.36
SP04B	5	441.5	2.26	22.97

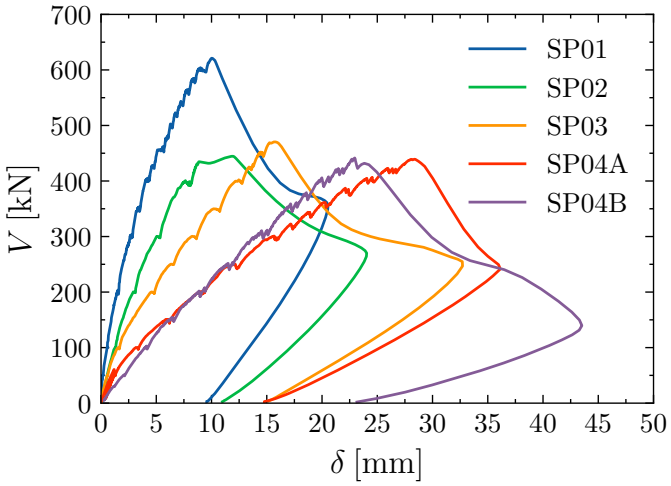

Figure 4.4: Load-displacement curves for all specimens (at the center of the loading plate).

4.2.2 Cracking pattern

The observed cracking patterns for all slab specimens are shown in Figure 4.5 with respect to top and bottom surfaces of the slab. The cracks in the top surface were almost parallel in the region close to the support, while they developed in a tangential manner close to the load introduction plate. Cracks in the bottom surface developed radially with respect to the load introduction plate.

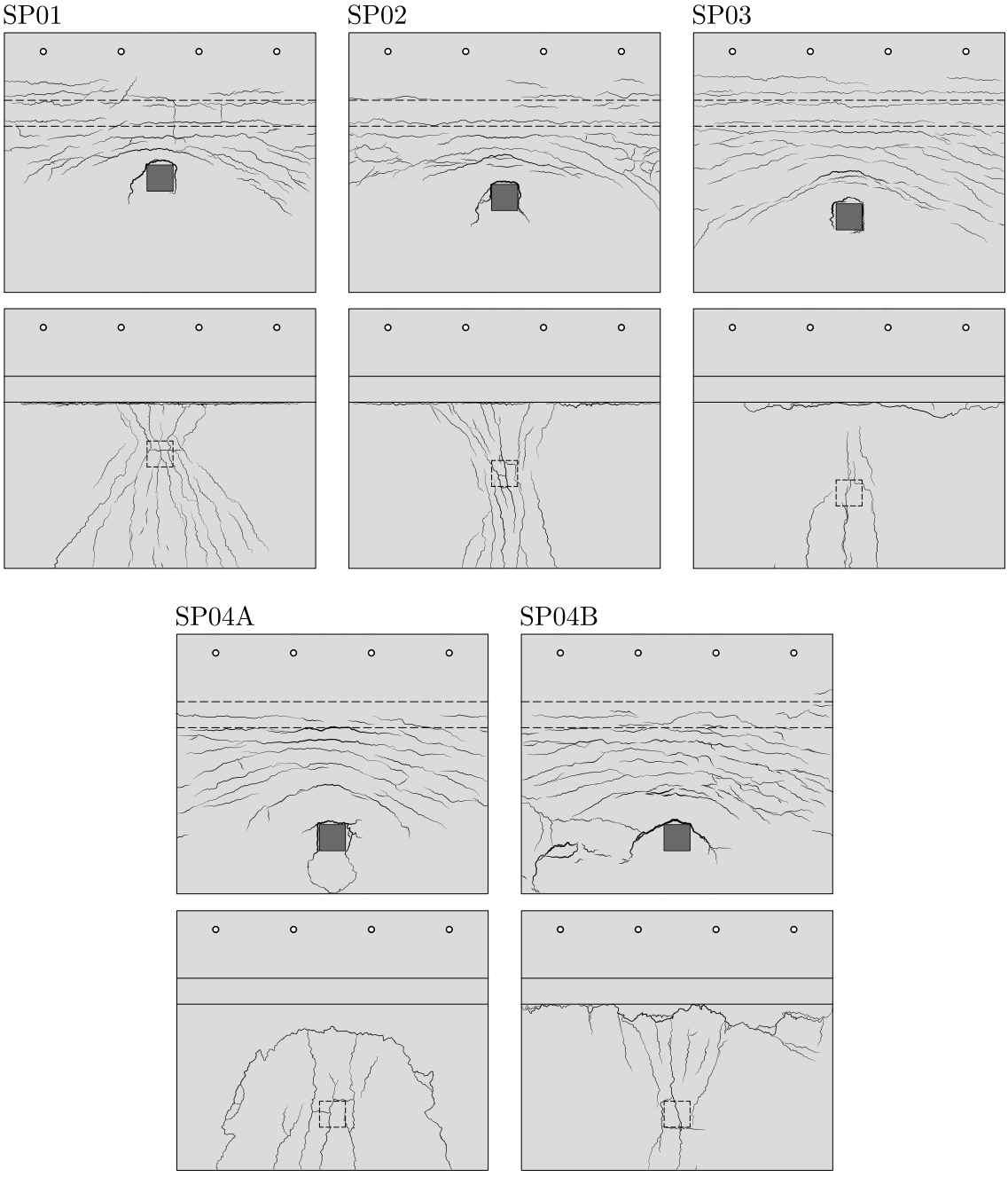

Figure 4.5: Top and bottom surfaces of cracking patterns after failure.

Chapter 5

Shear strength evaluation of bridge deck slabs

In this Chapter, the comparisons of the obtained test results from the eight experimental programmes are compared with calculated shear resistances according to the relevant models and selected methods presented in Chapter 3.

5.1 Database description

The database contains shear tests performed by: Vaz Rodrigues et al. [33], Rombach & Latte [30], Reissen & Hegger [28, 27], Natário et al. [26], Henze et al. [13, 29], Vida & Halvonik [34], Cantone et al. [5] and finally, the shear tests described in the Chapter 4 of this thesis.

5.2 Evaluation of a database by different calculation models

In case of the current EC2 model with French and Dutch approach for the assessment of shear capacity of reinforced concrete slabs under concentrated load, it is rather conservative for $a_v/d = 2$ and then the model's safety is gradually decreasing for higher values of a_v/d ratio. It shows a big scatter, which results in a large CoV = 0.41 and 0.33 for the Dutch and French approach, respectively (Figure 5.1(a) and (b)).

The best results were obtained with analytical approach by the Compression Chord Capacity Model (CCCM) method introduced by Marí et al. [21] and by the current EC2 modified with the model for the distribution of shear forces according to French approach with proposed limit for distance of the critical control section from the loaded area, as shown in Figure 3.2(a). High quality of these methods is given by

a very low value of CoV and an average value of the ratio V_{test}/V_{calc} close to one (Figure 5.1 (c) and (f)).

In the case of the *fib* Model Code 2010 model according to the Level-of-Approximation II (Figure 5.1 (d)), it was observed high safety level of the model for ratio $a_v/d = 2$, the average value reached 1.20. The model's deficiency is that the model safety level decreases with increasing value of a_v/d.

The ACI 318-19 approach (Figure 5.1 (e)) with the effective width determined according to the CCCM model provides much higher safety level in comparison with the modified French approach, while model's CoV is also slightly worse. Generally, the ACI 318-19 approach seems to be conservative even thought the proposed β factor and the maximum distance of the control section (Figure 3.4) are applied.

5.2.1 Linear finite element analysis

Better results are obtained by more refined approaches, where the internal forces are calculated by means of an uncracked linear-elastic finite element analysis (LFEA) (preferably with $\nu = 0$ and $G_c = E_c/16$ [26]). Such models are CSCT model and the proposed draft of the Eurocode 2 (prEC2).

Average value of the CSCT model is 1.00 and the CoV is only 12%. As the prEC2 model is based on the CSCT model, its results are also fairly accurate, except for the loads close to the support which are conservative because the enhancement factor of $\beta = a_v/2d$ is used. The accuracy of the both models is decreasing with the increasing ratio of a_v/d and this is because the model considers fixed section at the distance of $d/2$ from the face of the support.

The modification of the prEC2 enhancement factor is proposed as $\beta = a_v/2.75d$ and for the loads applied at effective shear span larger than $a_{cs} > 4d$, punching shear should be checked according to the following prEN 1992-1-1 equation:

$$\tau_{Rd,c} = 0.6 k_{pb} \left(100 \rho_l f_c \frac{d_{dg}}{d} \right)^{1/3} \leq 0.6 \sqrt{f_c} \tag{5.1}$$

$$k_{pb} = 3.6 \sqrt{1 - \frac{b_0}{b_{0,5}}} \leq 2.5 \tag{5.2}$$

where b_0 is the length of the perimeter at the face of the applied load and $b_{0,5}$ is the length of the control section located at $0.5d$ from the face of the loaded area. Three-sided control perimeter is proposed as shown in Figure 5.2.

Results with great accuracy are obtained by the proposed modification of the next generation of the Eurocode 2 (prEN 1992-1-1), with an average ratio of 1.06 and the lowest CoV along with CSCT model, of only 12%.

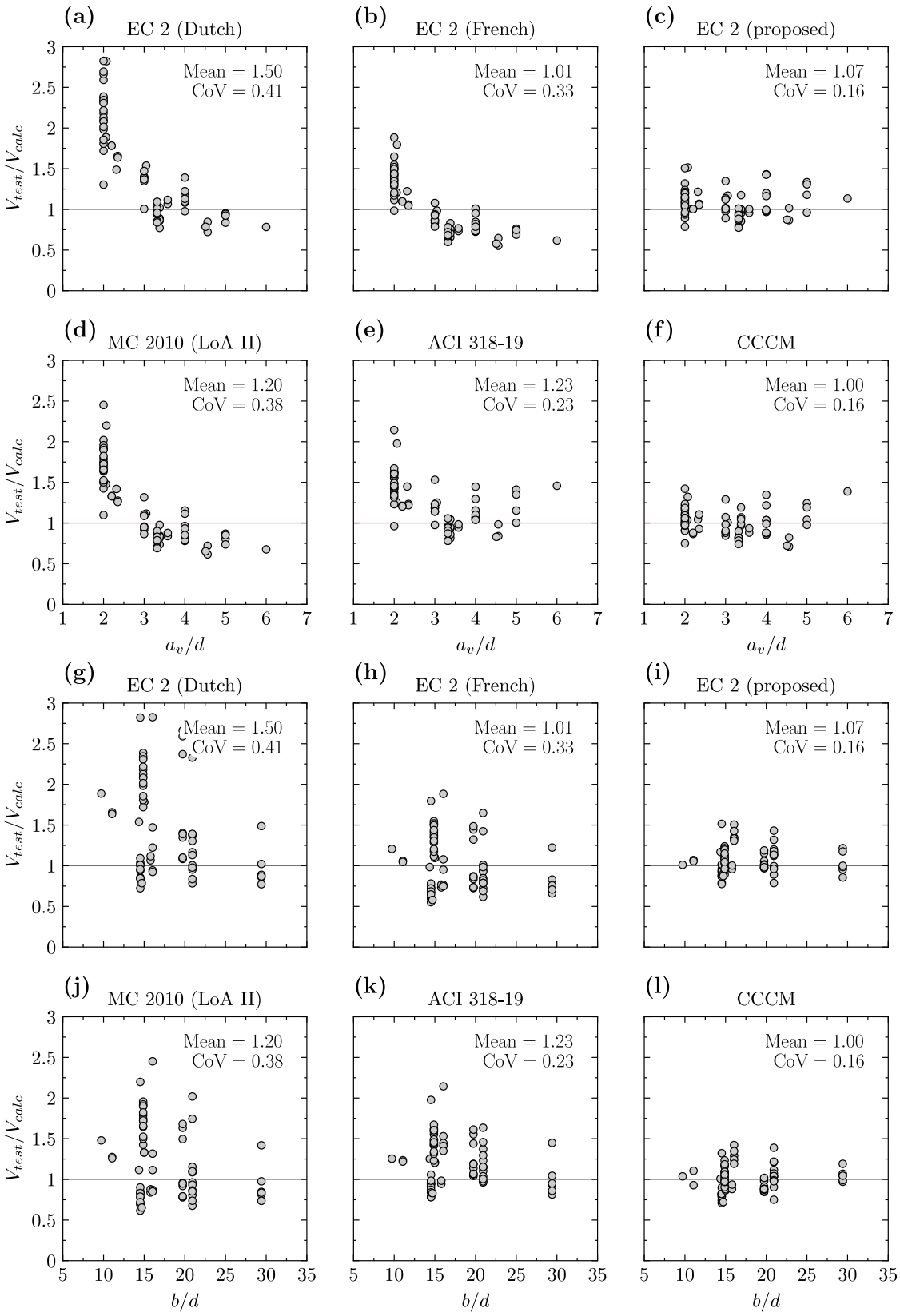

Figure 5.1: Comparison of a database results with different calculation models as a function of: **(a-f)** a_v/d; and **(g-l)** b/d.

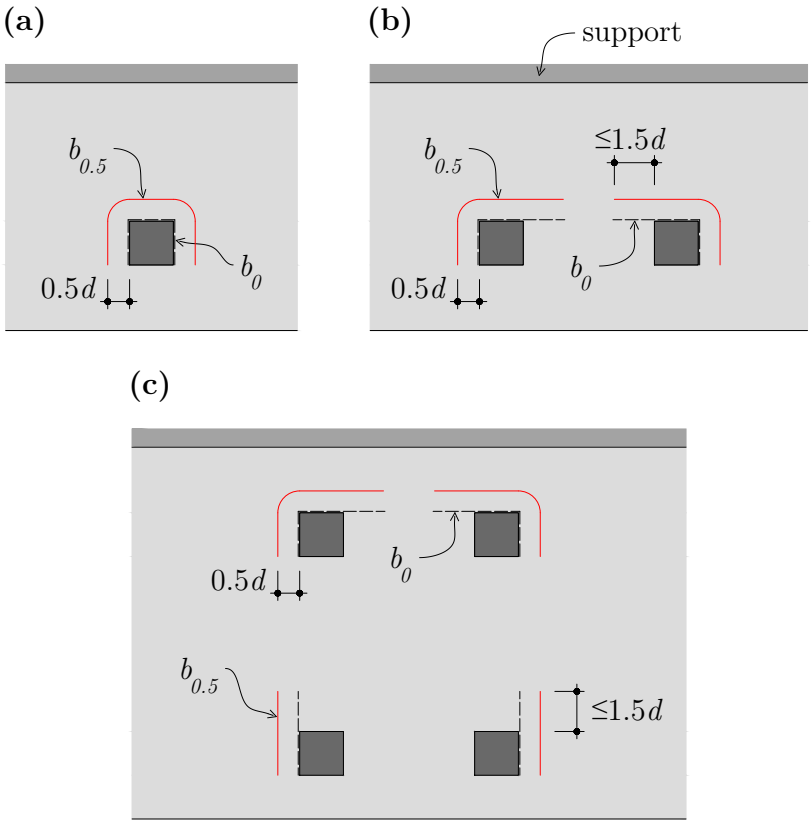

Figure 5.2: Proposed three-sided control perimeters for punching shear used with prEN 1992-1-1 [6] in the case of: **(a)** a single; **(b)** two; and **(c)** four concentrated loads.

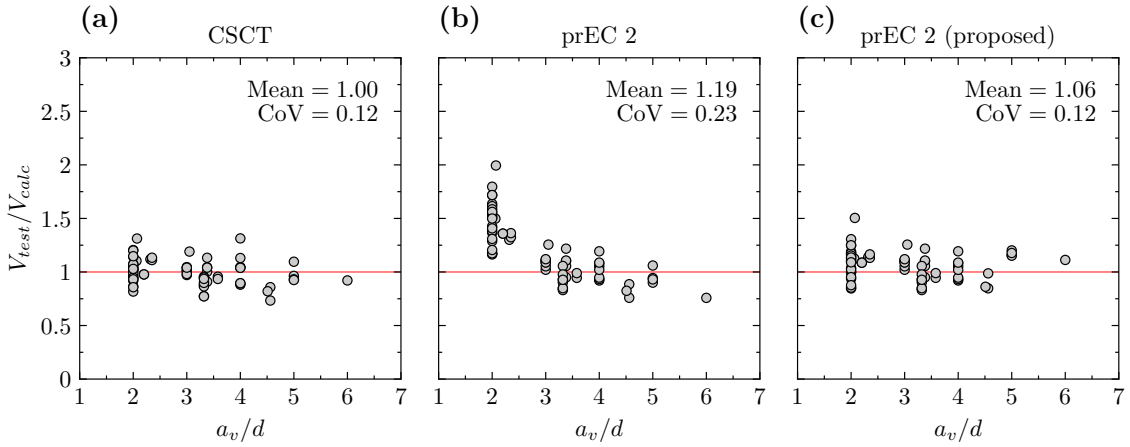

Figure 5.3: Comparison of a database results with different calculation models as a function of: **(a)** CSCT [24, 3]; **(b)** prEN 1992-1-1 [6]; and **(c)** proposed modification of prEN 1992-1-1.

Chapter 6

Numerical investigation

This Chapter describes the non-linear finite element analysis (NLFEA) procedures which were used to obtain a better understanding of the mechanics of shear failure of the previously tested specimens in Chapter 4.

6.1 General description of the numerical models

The three-dimensional view of the numerical model of the slab specimen and its components is show in Figure 6.1. Only a half of the slab was considered in the model, with appropriate boundary conditions on the plane symmetry.

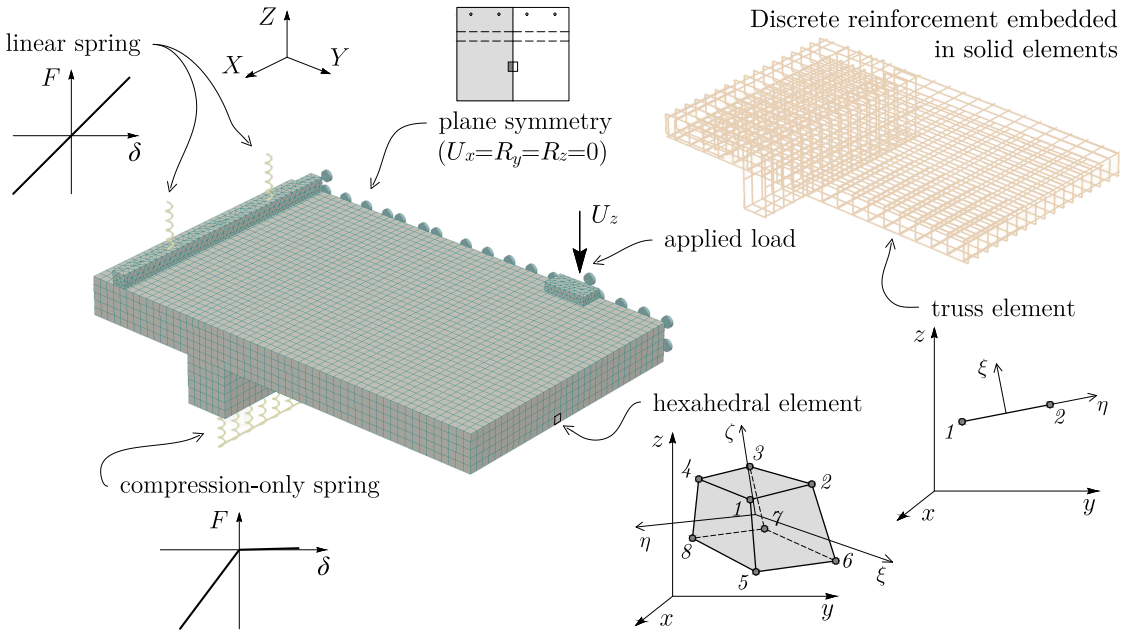

Figure 6.1: Continuum finite element model of the analysed slab specimens.

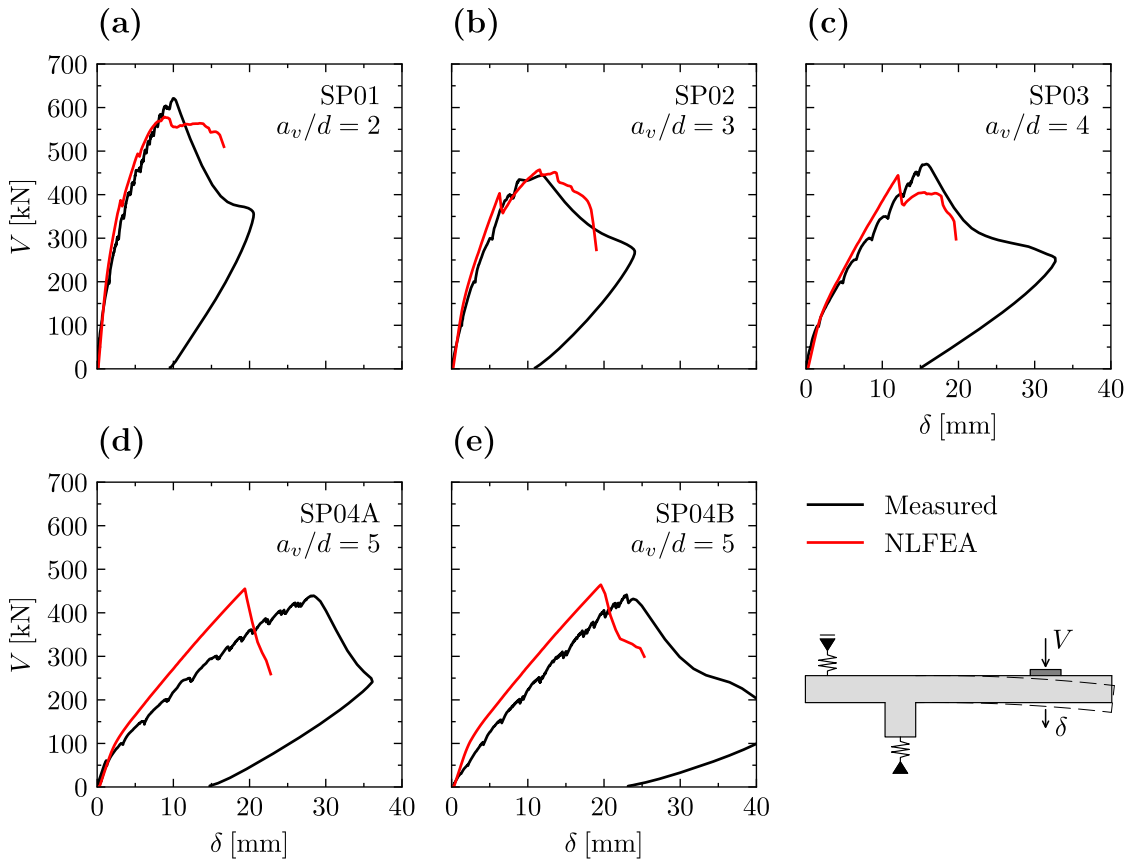

Figure 6.2: Comparison of measured and NLFEA load-displacement curves (at the center of the loading plate).

6.2 Results

The load-displacement relations obtained from the non-linear finite element analysis were compared to the corresponding relations obtained from experiments and are shown in Figure 6.2.

6.3 Parametric study

In this section, the calibrated finite element model was used to conduct a parametric study on the shear capacity of bridge deck slabs. The influence of several parameters, such as the influence of the concrete properties, the influence of the longitudinal and transverse reinforcement ratio, geometry of the slab and its loading configuration and finally the influence of the edge beam was studied.

For this purpose, the obtained shear capacities from NLFEA V_{NLFEA} were compared to a reference shear strength V_{ref} corresponding to the shear strength of SP02 slab with $a_v/d = 3$ obtained by NLFEA.

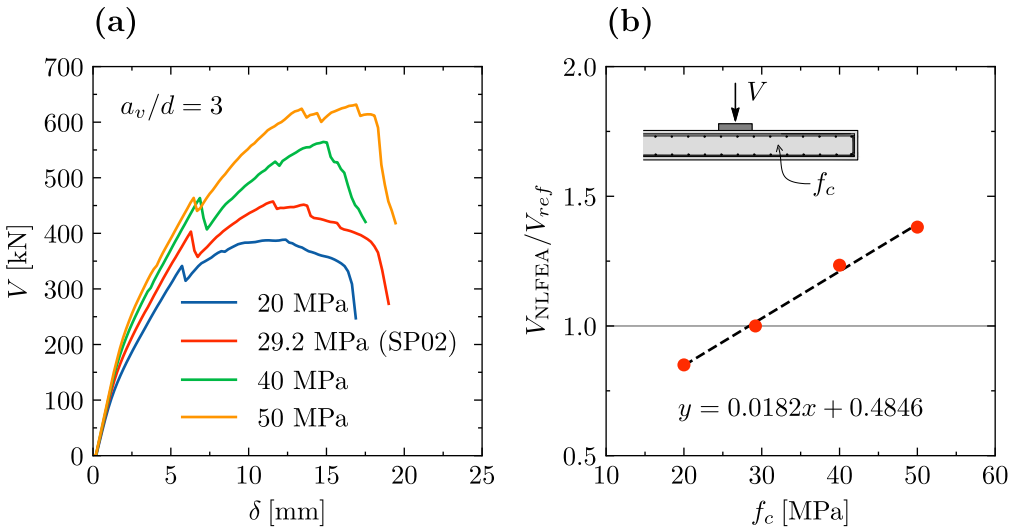

Figure 6.3: Effect of concrete compressive strength: **(a)** load-displacement curves; and **(b)** normalized shear resistance as a function of the concrete compressive strength f_c.

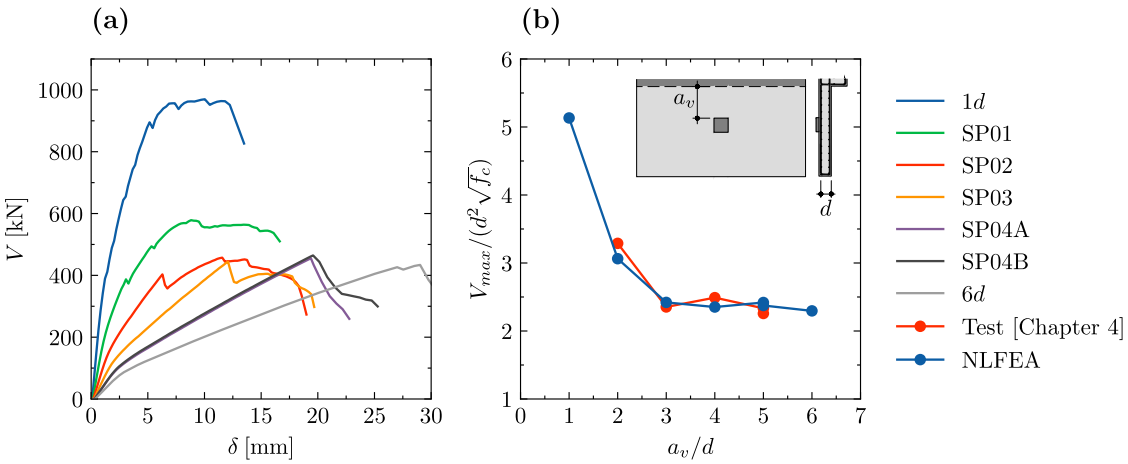

Figure 6.4: Effect of load position: **(a)** load-displacement curves; and **(b)** normalized shear resistance as a function of the shear span-to-depth ratio a_v/d.

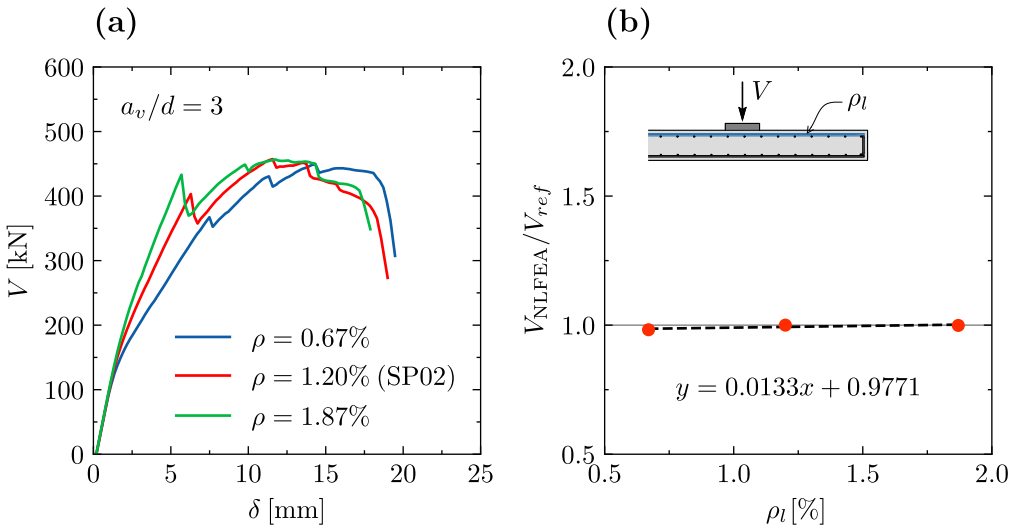

Figure 6.5: Effect of the main longitudinal reinforcement: **(a)** load-displacement curves; and **(b)** normalized shear resistance as a function of the reinforcement ratio ρ_l.

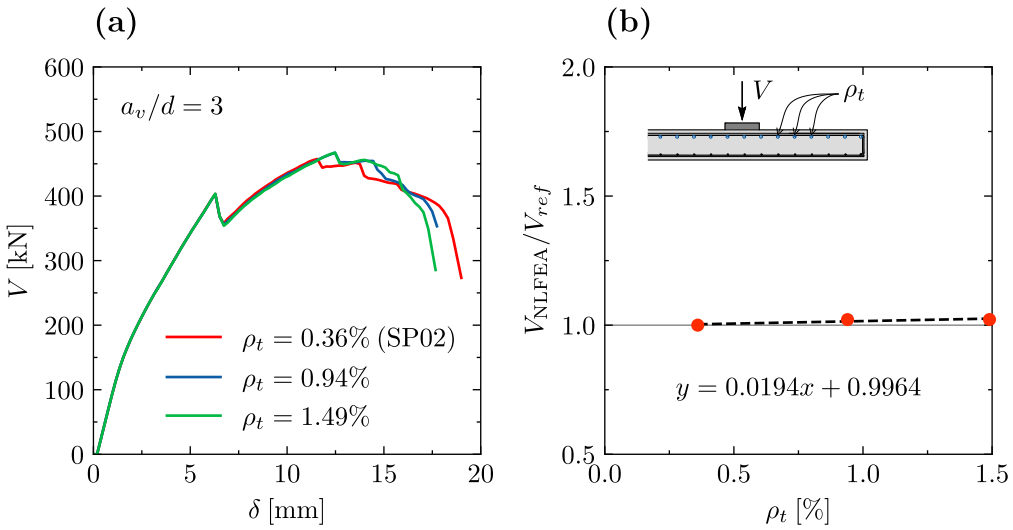

Figure 6.6: Effect of the top transverse reinforcement: **(a)** load-displacement curves; and **(b)** normalized shear resistance as a function of the reinforcement ratio ρ_t.

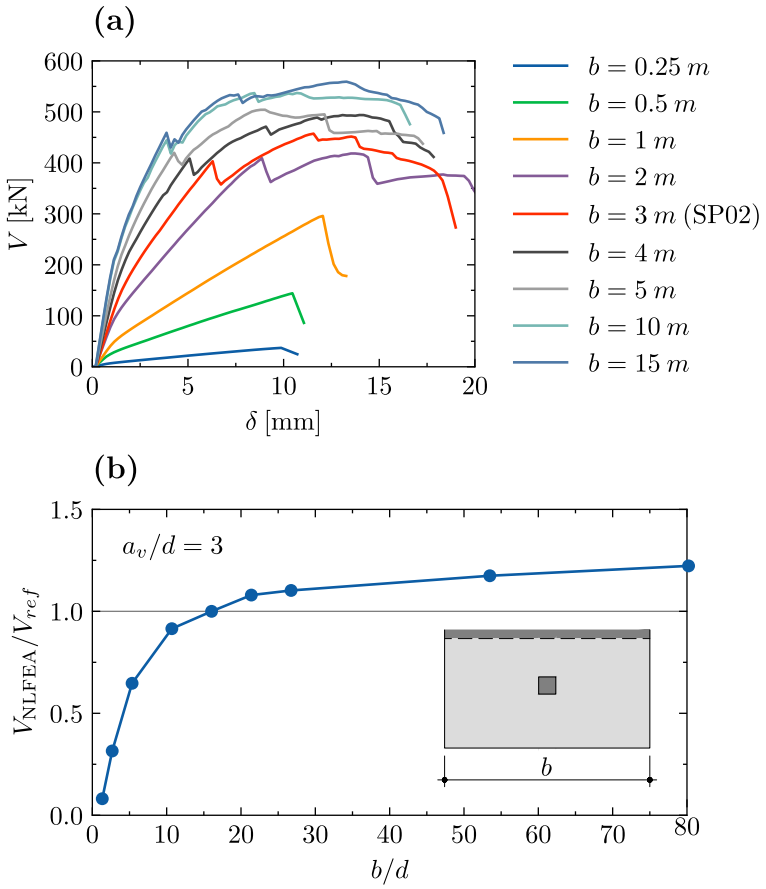

Figure 6.7: Effect of slab width: **(a)** load-displacement curves; and **(b)** normalized shear resistance as a function of the slab width-to-depth ratio b/d.

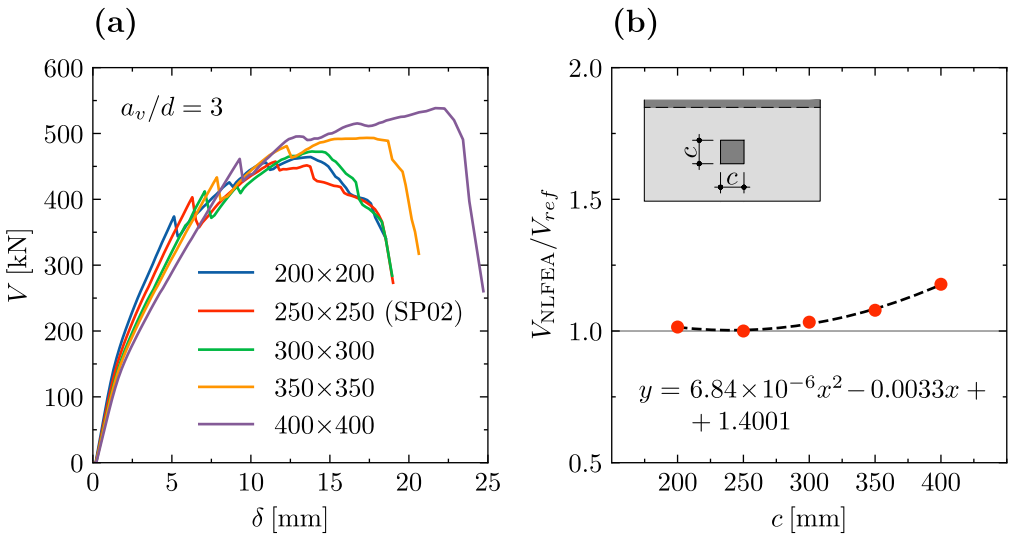

Figure 6.8: Effect of the size of the loading plate: **(a)** load-displacement curves; and **(b)** normalized shear resistance as a function of the size of the loading plate c.

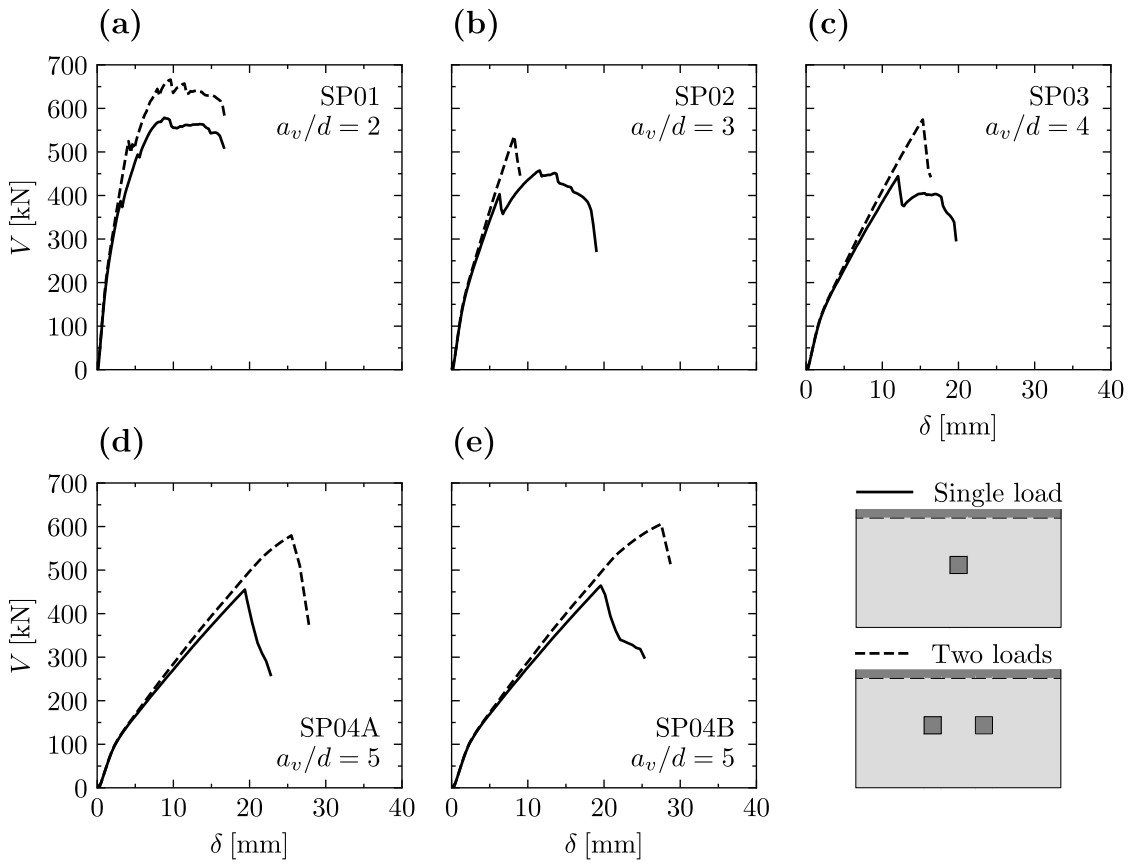

Figure 6.9: Load-displacement curves of the loading configuration with a single and two concentrated loads for: **(a)** SP01; **(b)** SP02; **(c)** SP03; **(d)** SP04A; and **(e)** SP04B specimen.

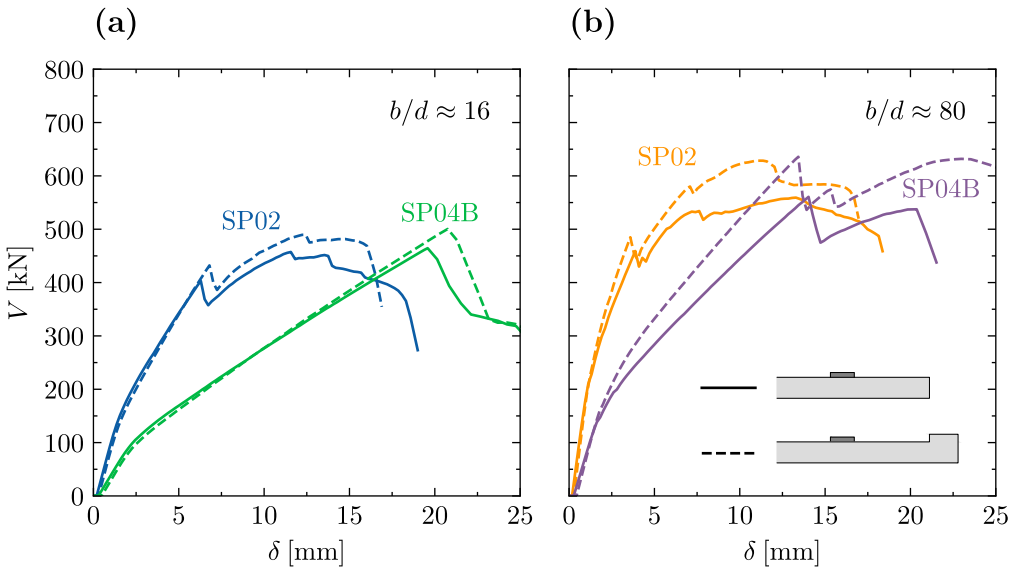

Figure 6.10: Influence of the edge beam for SP02 and SP04B specimen with slab width-to-depth ratio of: **(a)** $b/d \approx 16$; and **(b)** $b/d \approx 80$.

Chapter 7

Conclusions

This thesis presents an experimental, analytical and numerical investigation of shear resistance of cantilever slabs under concentrated load at different locations from the support. The investigation is supported by refined measurements performed on five reinforced concrete slabs subjected to a concentrated load.

7.1 Summary and conclusions

The main conclusions are listed below:

- The tests showed shear failure to be the governing failure mode for cantilevers representing the deck slabs of bridges. All slabs failed in shear and no flexural reinforcement yielding was reached;
- The safety of the current Eurocode 2 model is gradually decreasing as the load is applied further from the support. The proposed modification of the load spread model is on the safe side and gives much better results;
- The proposed modification of the next generation of the Eurocode 2 gives safe results with low scatter.
- Arching action seems to develop for free shear span up to approximately 2.75 times the effective flexural depth;
- For larger shear spans, punching shear should be also checked, instead of only one-way shear;
- The results of the tested slabs show significant redistribution of internal shear forces and bending moments, which is in contrast to beam tests;
- The results from the measurement demonstrate that the photogrammetry is an effective, accurate and suitable method for strain and displacement measurements during load tests.

7.2 Recommendations for practice

In the case of the current Eurocode 2 model, it is strongly recommended to use the load distribution angle according to the proposed modification of the French approach, where the control section is located at the distance at 2.0 times the effective flexural depth.

Practical rules for redistribution of internal forces based on the LFEA of the proposed modification of prEN 1992-1-1 are suitable for design and also for the assessment of existing bridge deck slabs.

7.3 Recommendations for further research

For further research, some propositions are presented:

- Tests on cantilever slabs under concentrated loads, varying the different parameters investigated in Section 6.3 of this thesis, in order to confirm the observations obtained by NLFEA.
- Post-tensioning is commonly introduced in bridge deck slabs of concrete box girder bridges to control the transverse tensile stresses induced by dead and live loads. Tests on post-tensioned cantilever slabs under concentrated load, in order to verify if there is an influence of the pre-stressing force on the shear strength and redistribution capacity of slabs;
- More tests with refined measurements of strain field by photogrammetry. This may allow for a detailed interpretation of the propagation of the failure surface and to better understand the response of the shear-critical regions;
- Fatigue tests on cantilever slabs under concentrated load.

Bibliography

[1] American Concrete Institute. *Building Code Requirements for Structural Concrete*. ACI 318-19. Farmington Hills, Michigan, USA, 2019, p. 623.

[2] Bažant, Z.P. "Size effect in blunt fracture: concrete, rock, metal". In: *Journal of engineering mechanics* Vol. 110, No. 4 (1984), pp. 518–535.

[3] Belletti, B., Scolari, M., Muttoni, A., and Cantone, R. "Shear strength evaluation of RC bridge deck slabs according to CSCT with multi–layered shell elements and PARC_CL Crack Model". In: *IABSE Conference Geneva 2015* (2015), pp. 1158–1165.

[4] Bentz, E.C., Vecchio, F.J., and Collins, M.P. "Simplified modified compression field theory for calculating shear strength of reinforced concrete elements". In: *ACI Structural Journal* Vol. 103, No. 4 (2006), pp. 614–624.

[5] Cantone, R., Fernández Ruiz, M., and Muttoni, A. "Shear force redistributions and resistance of slabs and wide beams". In: *Structural Concrete* Vol. 22, No. 4 (2021), pp. 2443–2465.

[6] CEN. *Draft of Eurocode 2: Design of concrete structures - Part 1-1: General rules - Rules for buildings, bridges and civil engineering structures*. prEN 1992-1-1:2021-09. Brussels: European Committee for Standardization, 2021, p. 375.

[7] CEN. *Eurocode 1: Actions on structures - Part 2: Traffic loads on bridges*. EN 1991-2. Brussels: European Committee for Standardization, 2003, p. 168.

[8] CEN. *Eurocode 2: Design of concrete structures - Part 1-1: General rules and rules for buildings*. EN 1992-1-1. Brussels: European Committee for Standardization, 2005, p. 229.

[9] Chauvel, D., Thonier, H., Coin, A., and Ile, N. "Shear resistance of slabs not provided with shear reinforcement". In: *CEN/TC* Vol. 250, (2007), p. 32.

[10] Drucker, D.C. "On structural concrete and the theorems of limit analysis". In: *International Association for Bridge and Structural Engineering* Vol. 21, (1961), pp. 45–59.

[11] Fédération Internationale du Béton. *fib Model Code for Concrete Structures 2010*. Germany: Ernst & Sohn, 2013, p. 434.

[12] Fernández, P.G., Marí, A., and Oller, E. "Theoretical prediction of the shear strength of reinforced concrete slabs under concentrated loads close to linear supports". In: *Structure and Infrastructure Engineering* Vol. 0, No. 0 (2021), pp. 1–14.

[13] Henze, L., Rombach, G.A., and Harter, M. "New approach for shear design of reinforced concrete slabs under concentrated loads based on tests and statistical analysis". In: *Engineering Structures* Vol. 219, (2020), p. 110795.

[14] Kani, G.N.J. "The riddle of shear failure and its solution". In: Vol. 61, No. 4 (1964), pp. 441–468.

[15] Kani, M.W, Huggins, M.W., and Wittkopp, R.R. *Kani on shear in reinforced concrete*. Canada: Deptartment of Civil Engineering, University of Toronto, 1979, p. 97.

[16] Kupfer, H.B. and Gerstle, K.H. "Behavior of concrete under biaxial stresses". In: *Journal of the engineering mechanics division* Vol. 99, No. 4 (1973), pp. 853–866.

[17] Lantsoght, E.O.L., van der Veen, C., and Walraven, J.C. "Shear in one-way slabs under concentrated load close to support". In: *ACI Structural Journal* Vol. 110, No. 2 (2013), pp. 275–284.

[18] Latte, S. "Zur Tragfähigkeit von Stahlbeton-Fahrbahnplatten ohne Querkraftbewehrung (in German) [Shear capacity of concrete bridge decks without transverse reinforcement]". PhD thesis. Technische Universität Hamburg, 2010, p. 181.

[19] Leahy, C., O'Brien, E., and O'Connor, A. "The effect of traffic growth on characteristic bridge load effects". In: *Transportation Research Procedia* Vol. 14, (2016), pp. 3990–3999.

[20] Leonhardt, F. and Walther, R. *Schubversuche an einfeldrigen Stahl-betonbalken mit und ohne Schubbewehrung (in German) [Shear tests on beams with and without shear reinforcement]*. 151. Berlin, Germany: Ernst, 1962, p. 83.

[21] Marí, A., Bairán, J., Cladera, A., Oller, E., and Ribas, C. "Shear-flexural strength mechanical model for the design and assessment of reinforced concrete beams". In: *Structure and Infrastructure Engineering* Vol. 11, No. 11 (2014), pp. 1399–1419.

[22] Muttoni, A. "Punching shear strength of reinforced concrete slabs without transverse reinforcement". In: *ACI Structural Journal* Vol. 105, No. 4 (2008), pp. 440–450.

[23] Muttoni, A. and Fernández Ruiz, M. "Levels-of-approximation approach in codes of practice". In: *Structural Engineering International* Vol. 22, No. 2 (2012), pp. 190–194.

[24] Muttoni, A. and Fernández Ruiz, M. "Shear strength of members without transverse reinforcement as function of critical shear crack width". In: *ACI Structural Journal* Vol. 105, No. 2 (2008), pp. 163–172.

[25] Natário, F. “Static and fatigue shear strength of reinforced concrete slabs under concentrated loads near linear supports”. PhD thesis. Lausanne: IIC, 2015, p. 201.

[26] Natário, F., Fernández Ruiz, M., and Muttoni, A. “Shear strength of RC slabs under concentrated loads near clamped linear supports”. In: *Engineering Structures* Vol. 76, (2014), pp. 10–23.

[27] Reissen, K. and Hegger, J. “Experimental investigations on the effective width for shear”. In: *Maintenance, Monitoring, Safety, Risk and Resilience of Bridges and Bridge Networks - Proceedings of the 8th International Conference on Bridge Maintenance, Safety and Management, IABMAS 2016* (2016), pp. 2340–2348.

[28] Reissen, K. and Hegger, J. “Experimental investigations on the shear capacity of RC slabs under concentrated loads - Influence of degree of restraint and Moment-Shear Ratio”. In: *Concrete - Innovation and Design: fib Symposium Proceedings* (2015), pp. 68–69.

[29] Rombach, G. and Henze, L. “Shear capacity of concrete slabs without shear reinforcement under concentrated loads close to support”. In: *High Tech Concrete: Where Technology and Engineering Meet - Proceedings of the 2017 fib Symposium* (2017), pp. 676–683.

[30] Rombach, G.A. and Latte, S. “Shear resistance of bridge decks without shear reinforcement”. In: *Proceedings of the International FIB Symposium 2008 - Tailor Made Concrete Structures: New Solutions for our Society* (2008), pp. 519–525.

[31] Sigrist, V., Bentz, E., Fernández Ruiz, M., Foster, S., and Muttoni, A. “Background to the fib Model Code 2010 shear provisions – part I: beams and slabs”. In: *Structural Concrete* Vol. 14, No. 3 (2013), pp. 195–203.

[32] Vaz Rodrigues, R. “Shear strength of reinforced concrete bridge deck slabs”. PhD thesis. Lausanne: IS, 2007, p. 289.

[33] Vaz Rodrigues, R., Fernández Ruiz, M., and Muttoni, A. “Shear strength of R/C bridge cantilever slabs”. In: *Engineering Structures* Vol. 30, No. 11 (2008), pp. 3024–3033.

[34] Vida, R. and Halvonik, J. “Tests of shear capacity of deck slabs under concentrated load”. In: *Proceedings of the 12th fib International PhD Symposium in Civil Engineering* (2018), pp. 773–779.

[35] Zsutty, T.C. “Beam shear strength prediction by analysis of existing data”. In: *ACI Journal Proceedings* Vol. 65, No. 11 (1968), pp. 943–951.